ISSN: 0975-8585

Research Journal of Pharmaceutical, Biological and Chemical Sciences

# Catalytic Properties of Bimetallic Au@Ag Core@Shell Nanoparticles; Effect of Shell thickness.

**Wael H Eisa[a,*], Emad Al-Ashkar[a], SM El-Mossalamy[b], and Safaa SM Ali[a].**

[a]Spectroscopy Department, Physics Division, National Research Centre (NRC), Egypt.
[b] Physics Department, Faculty of Science, Girls Branch, Al-Azhar University, Cairo, Egypt.

**ABSTRACT**

Noble metal nanocomposites have attracted the attention of the researchers in the field of catalysis owing to their unique properties, which are directly related to their sizes and shapes. The catalytic properties of Au@Ag core@shell nanocomposites are studied on the degradation of 4-nitrophenol (4-NP) as model reaction. The prepared nanocomposites are characterized using Uv-visible spectroscopy, transmission electron microscopy (TEM), dynamic light scattering (DLS), and zeta analyzer. TEM images confirm the increase of a thin coating of Ag shell around Au core in a core@shell structure.

**Keywords;** Noble metals; catalysis; 4-nitrophenol; Uv-vis; zeta potential

***Corresponding author***

ISSN: 0975-8585

## INTRODUCTION

One of the mainly important topics in scientific literatures is the removal of water pollutants [1-3]. This strongly enforces the development of new high performance catalytic materials. Among various kinds of noble metals, Gold and Silver nanoparticles have a great deal of attention in the field of catalytic degradation of water pollutants because of its well-known catalytic activity, optical properties and chemical functionability [4-5]. Removing water pollutants using zero valent gold or silver nanoparticles motivate researchers because of numerous benefits such as increasing rate of reaction and efficiency, mild reaction conditions, and requisite for minimal follow-up treatment [6].

Bimetallic nanocomposites have attracted intensive interest due to their novel optical, electronic, sensing and catalytic properties. The developed physiochemical and surface properties of bimetallic nanoparticles may be attributed to combinational interactions between the electronic states of the two metals which are different from individual metals [7-8]. Gold@silver (Au@Ag) core@shell nanocomposites emerged as the most common bimetallic nanostructures due to their plasmonic, catalytic and sensor based applications. The physiochemical characteristics of these core@shell nanocomposites solely depend on the dimension of core and shell and on the composition [9-11].

4-Nitrophenols (4-NP) are highly toxic and mutagenic pollutants which have damage effect on the central nervous system, kidney, liver and blood. 4-NP and their derivatives are widely used in chemical industries for the production of drugs, insecticides, fungicides, and explosives. 4-NP is characterized by its solubility and stability in water so it stays a very long time without degradation [12]. This accumulation increases the environmental issues due to the carcinogenic activities of 4-NP [13]. Several techniques have been used for the removal of nitrophenols from water [14-16] but these methods are energy consuming and use organic solvents. The use of the nanoparticles as catalysts to reduce 4-NP into 4-aminopenol (4-AP) is considered as an easy, fast and energy saving process [2, 17, 18]. On the other hand, 4-aminophenol is an environmentally safe end product due to it is an important intermediate for the production of analgesic and antipyretic drugs.

In this work, the catalytic properties of Au@Ag core@shell nanocomposites are studied on the degradation of 4-nitrophenol (4-NP) as model reaction. This bimetallic nanoparticles are prepared by self-seeding route using polyvinylpyrrolidone (PVP) as both reducing and stabilizing agent in one step reaction[19]. UV-visible spectroscopy, transmission electron microscopy (TEM), dynamic light scattering (DLS), and zeta analyzer tools are used for characterizing the prepared Au@Ag core@shell nanocomposites to show the effect of Shell thickness on the degradation process.

## MATERIALS AND EXPERIMENTAL METHODS

### Materials.

Gold chloride, hydrate ($H(AuCl_4).H_2O$) was Purchased from Electron Microscopy Sciences Inc. Silver nitrate ($AgNO_3$) and PVP (Mw= 40,000 g/mol) were obtained from Bio Basic Inc. All precursors are of high analytical purity and used as received.

### Preparation of Au@Ag core@shell nanocomposites

Au@Ag core@shell nanocomposites were prepared via self-seeding process in one step reaction. 100 µl of $H(AuCl_4).H_2O$ ($10^{-2}$ M) were injected to 0.1 g of PVP powder and mixed thoroughly within agate mortar until a homogenous paste was obtained. Subsequently, different volumes of $AgNO_3$ ($10^{-1}$ M) were added to the above paste with continuous grinding to achieve good dispersion of the $Ag^+$ ions within the polymeric paste. The reaction was kept in darkness to avoid photoreduction. The polymeric paste solidified after 4-6 h and the reaction stopped completely [19].

### Instrumentations

The UV-vis absorption spectra were collected using V-630 UV–VIS spectrophotometer (Jasco, Japan). The size and morphology of the prepared Au@Ag cor@shell were investigated using transmission electron

microscopy (TEM) of the type JEM-2100 (JEOL, Japan). Zetapotential measurements were performed with dynamic light scattering instrument (Zetasizer Nano series, Malvern Instruments Ltd).

**Catalytic activity of Au@Ag core@shell nanocomposites in degradation of 4-nitrophenol**

For studying the catalytic activity of as-prepared Au@Ag core@shell nanocomposites, the reduction of 4-NP to 4-aminophenol by NaBH4 is performed as a probe reaction. The effect of shell thickness on the speed of catalytic reduction is studied using the Au@Ag core@shell nanocomposites colloids prepared with 4 different quantities of $AgNO_3$ amounts (25, 50, 75 and 100 µL). The method reported by Narayanan and Sakthivel [2] was applied here but with using smaller volumes of Au@Ag core@shell nanocomposites colloids. In standard quartz cell with a 1-cm path length, 2.77 mL of water was mixed with 25 µL ($10^{-2}$ M) of 4-NP solution and 200 µL of freshly prepared NaBH4 solution ($10^{-1}$ M). Thereafter, 50 µL of Au@Ag core@shell nanocomposites solution was added to the above mixture. After the addition of Au@Ag core@shell nanocomposites colloid, reduction is ascertained by recording the UV–vis spectra.

## 3. RESULTS AND DISCUSSION

**Optical properties**

Gold and silver NPs are extremely studied due to their strong surface plasmon resonance (SPR) in the visible spectrum. The growth of these nanoparticles will reflect in a presumed color change that serves as an indicator for structural and morphological changes[20]. This advantage can be detected with the naked eye only. Fig.1 shows the color change of the investigated samples from violet to brown upon the addition of the different volumes of $AgNO_3$ solution.

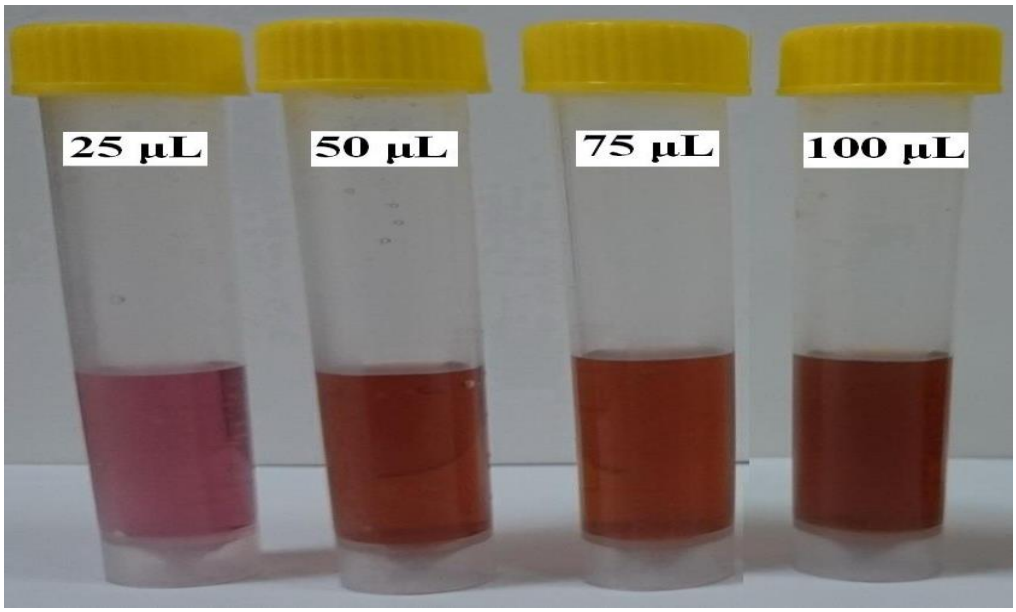


**Fig. 1 The color variation of Au@Ag core@shell as a result of $AgNO_3$ addition in different volumes**

The above observations are consistent with the results obtained by the UV-vis spectra of the Au@Ag core@shell given in Fig. 2. It can be seen that the characteristic SPR band of Au NPs at 520 nm are blue-shifted to a sharp peak at 455 nm of increased intensity due to the addition of $Ag^+$ ions (25-100 µl). This is attributed to morphological changes in which the PVP chains are used for the controlled reduction of $Ag^+$ ions and thereby deposition of Ag-shell over the Au-core[19]. With the successive deposition of reduced Ag NPs, a single absorption band at 455 nm having a brown color appeared i.e. the incident ray could only penetrate the Ag shell of a certain thickness and could not arrives Au cores to excite their electrons. Therefore, it is supposed that Ag NPs completely surround Au NPs giving rise to $Au_{core}$-$Ag_{shell}$ (Au@Ag core@shell).

ISSN: 0975-8585

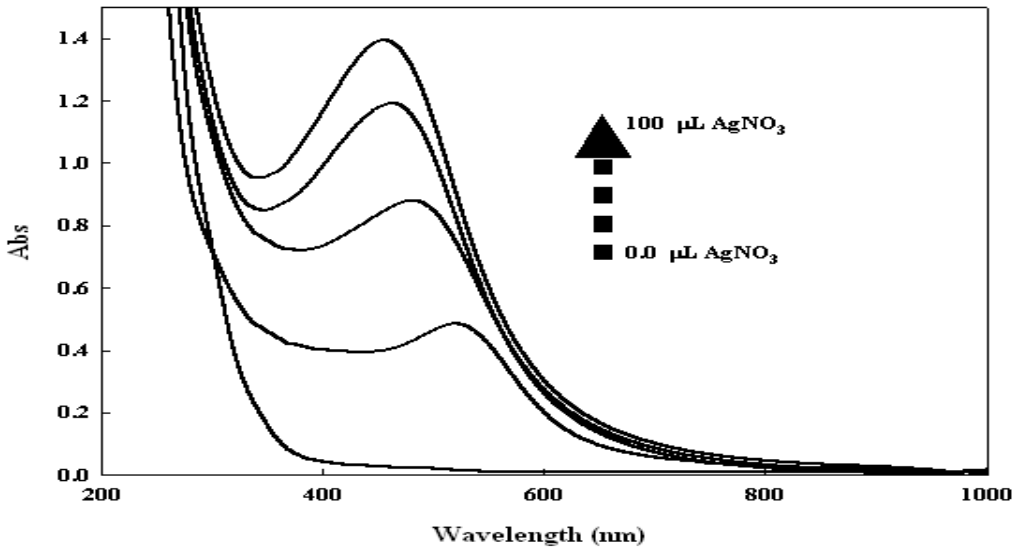


**Fig. 2 The absorption spectra of the Au@Ag core@shell prepared using increasing amounts of $AgNO_3$ (25-100) µL.**

**TEM analysis**

Typical TEM images of the synthesized Au@Ag core@shell using 25, 50, 75, and 100 µL of 0.1 M $AgNO_3$ have been shown in Fig. 3. It is clear from the TEM images that the Au@Ag core@shell nanocomposites are spherical in shape. The size of the gold core is not affected considerably while the thickness of Ag shell is increased gradually with the increasing amount of $AgNO_3$ used.

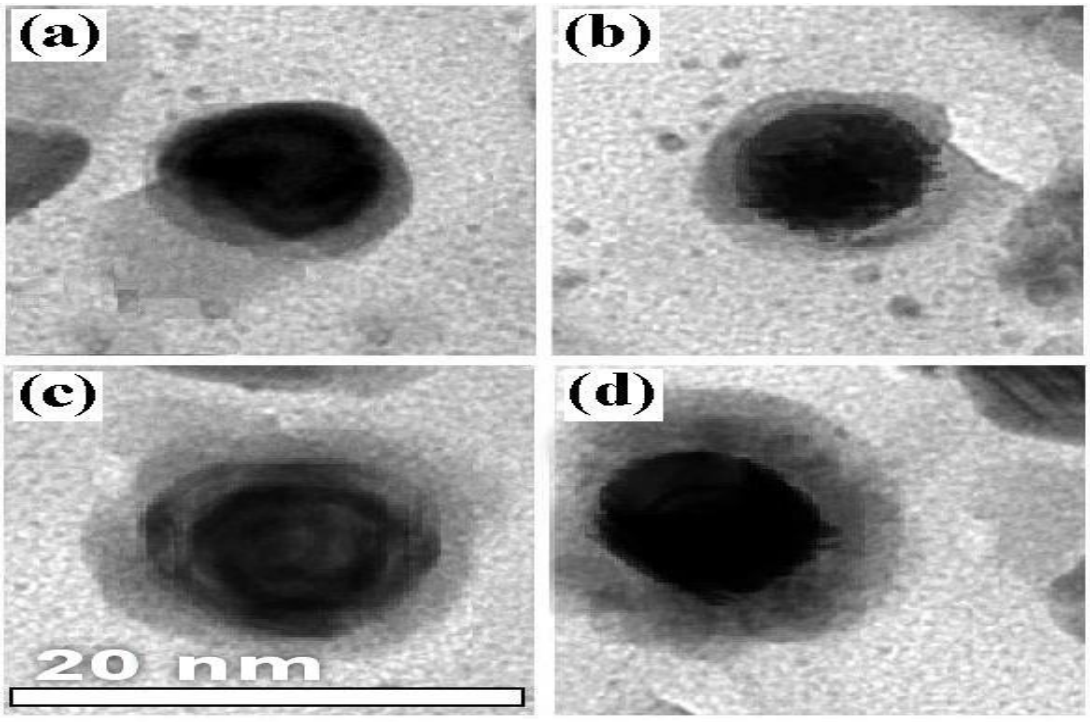


**Fig. 3 TEM images of (a) Au@Ag25, (b) Au@Ag50, (c) Au@Ag75, and (d) Au@Ag100 bimetallic core@shell nanocomposites.**

**DLS analysis**

The particle size and size distribution can also be measured with a dynamic light scattering which utilizes the electromagnetic waves scattered through a particle suspension to extract the size-related

ISSN: 0975-8585

information. The size distributions of Au@Ag core@shell are shown in Fig. 4. The particle size is displayed in x-axes with logarithmic scale. The DLS data shows that the sizes of Au@Ag core@shell increase by increasing the $AgNO_3$ amount, which is consistent with the results observed in UV-vis spectra (Fig. 2).

The particle size determined using DLS technique is larger than the value obtained from TEM images. The disagreement of particle size measurement by the two methods is quite common in other materials [21]. The TEM image analysis provides direct value of the particle-diameter, while DLS gives the hydrodynamic radius. The hydrodynamic radius is that of a theoretical sphere that has the same diffusion rate within the same viscous medium being measured. This diameter is not only related to the diameter of the nanoparticles (as in the case of TEM technique) but it is also related to all precursors adsorbed on the nanoparticles surface (e.g., solvents, surfactants ….etc.) and the thickness of the electrical double layer around the particle. As a result, the diameter measured in DLS technique is quite larger than that obtained by TEM [22].

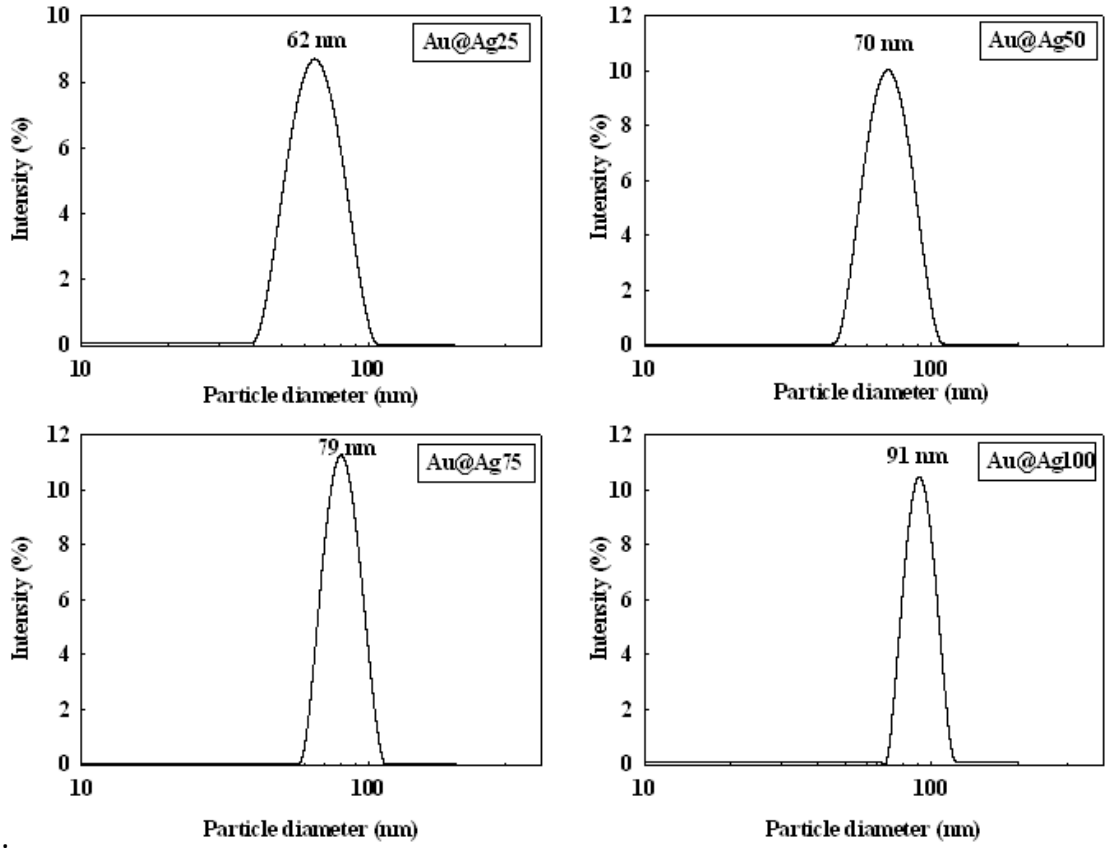


**Fig. 4 the particle size distribution estimated by DLS of PVP stabilized Au@Ag core@shell prepared with different amounts of $AgNO_3$.**

**Zeta potential**

Zeta potential measurements are performed to determine the surface charge of the PVP-capped Au@Ag core@shell nanocomposites. Such measurements help in understanding the stability of Au@Ag core@shell colloids in a dielectric medium. As given in Fig. 5, a freshly prepared solution of Au@Ag25 displays a prominent n-band at -12 mV at 7.5 pH. The value of zeta potential is increased to -18, -19, and -24 mV with the continuous addition of 50, 75 and 100 µL of $AgNO_3$, respectively.

Negative values of the zeta potential imply formation of the negative charges on the surface of the Au@Ag core@shell nanocomposites. When PVP-capped Au@Ag core@shell approach towards each other, the negatively charged surface of the nanocomposites prevents aggregations and hence increases the solution stability by electrostatic repulsion effect. The adsorbed PVP with extended vinyl backbone chain prevents the agglomeration by steric hindrance [23, 24].

ISSN: 0975-8585

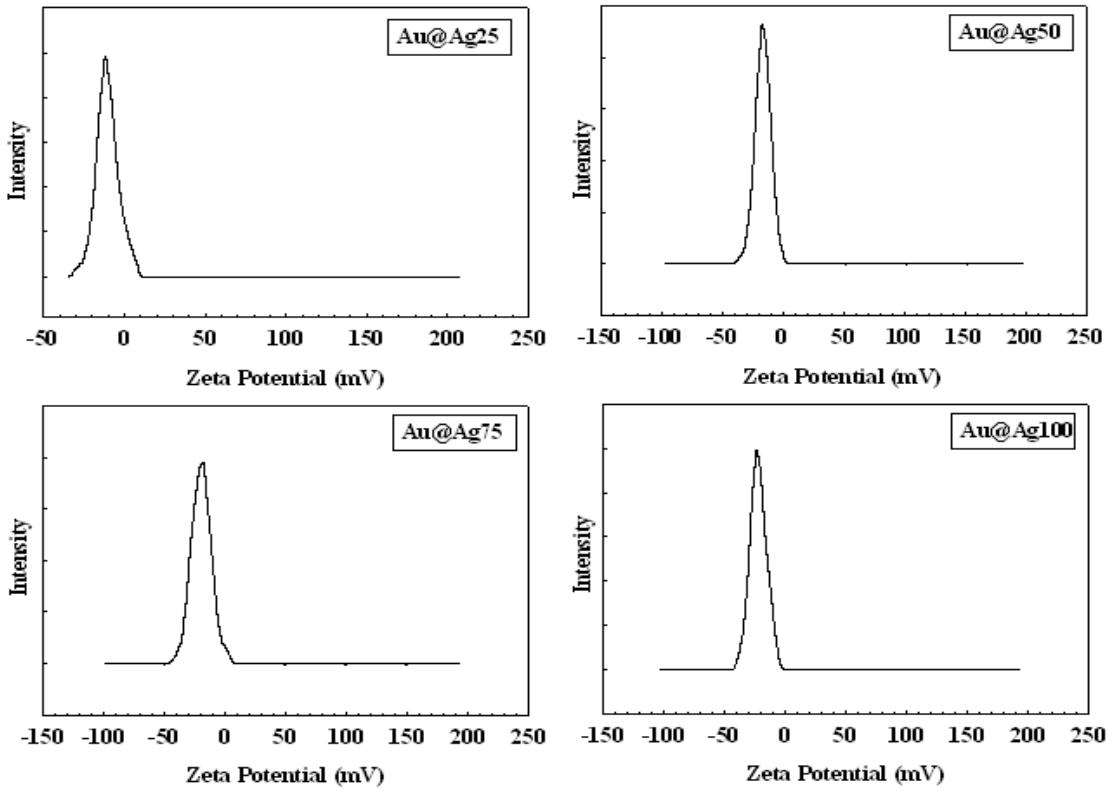


**Fig. 5 Zeta potential of a Au@Ag core@shell nanocomposites prepared with different amounts of $AgNO_3$.**

**Catalytic properties of Au@Ag core@shell nanocomposites**.

To monitor the effect of shell thickness on the physical properties, we have evaluated the catalytic activities of Au@Ag core@shell nanocomposites in the reduction reaction of 4-nitrophenol (4-NP) using $NaBH_4$ to form 4-aminophenol (4-AP). The reduction of 4-NP to 4-AP proceeds via an intermediate 4-nitrophenolate ion formation[25].

Fig. 6 shows the absorption spectra of 4-NP before and after addition of the reducing agent ($NaBH_4$). The aqueous solution of 4-NP is colorless and exhibit maximum absorption at 317 nm. After the addition of $NaBH_4$, the color of the solution changes from colorless to yellow and the absorption spectrum shows an intense absorption band at 398 nm. This is considered as an indication to the formation of 4-nitrophenolate ions[26].

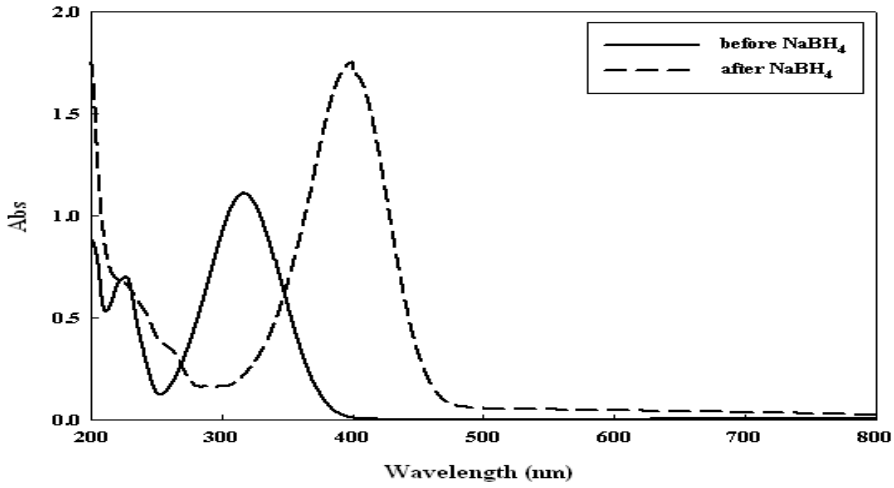


**Fig. 6 the absorption spectra of the 4-NP before and after addition of the reducing agent $NaBH_4$**

ISSN: 0975-8585

The reduction reaction of 4-NP to 4-AP using $NaBH_4$ is thermodynamically favorable. However, the large difference between the reduction potential of 4-NP/4-AP (−0.76 V) and that of $H_3BO_3/BH_4^-$ (−1.33 V), make this reaction is not kinetically favored [27]. Hence, we follow the reaction between 4-NP and $NaBH_4$ in the absence of the nanocatalyst thereby monitoring the profile of the absorption peak at 400 nm for 48 h. It is observed that the 400 nm-absorption peak maintains its position, shape and intensity without considerable changes. Furthermore, no new peaks are recorded within the investigated spectral range. This confirms that this reaction does not occur in absence of the nanocatalyst.

After addition of Au@Ag core@shell to the reaction medium, the reaction proceeds easily (see Fig. 7). The 400 nm absorption peak of 4-NP suffered from a gradual decrease in the intensity accompanied by an evolution of a new absorption peak at 298 nm which is related to the formation of 4-AP according to equation 1. The reaction progress is followed by recording the absorption peak at 400 nm of 4-NP and that at 298 nm of 4-AP as a function of time.

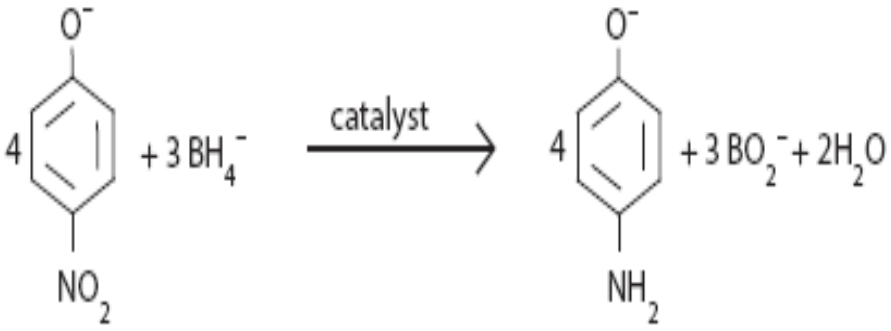


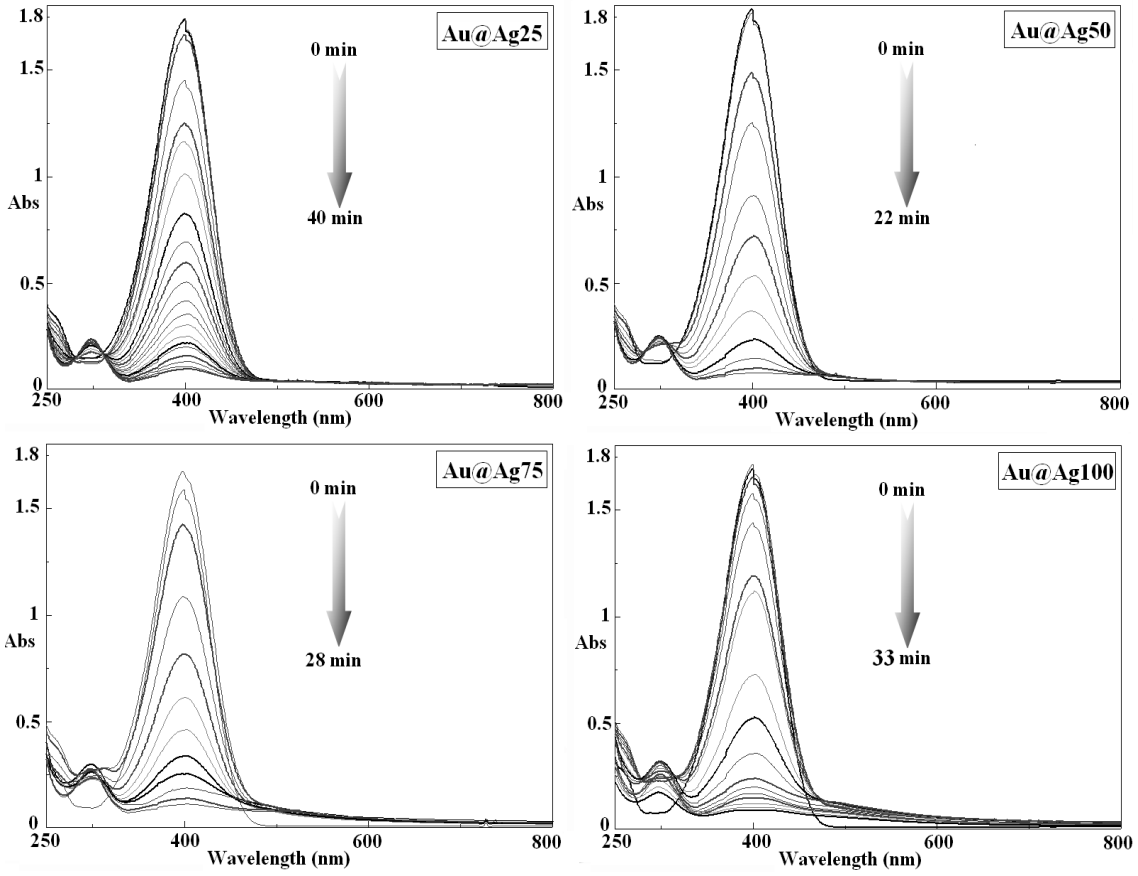


**Fig.7 the time evolution of the absorption spectra for the degradation of 4-NP using $NaBH_4$ as reducing agent in presence of Au@Ag core@shell with different shell thicknesses**

ISSN: 0975-8585

It is seen from Fig. 7 that the intensity of the absorption peak of 4-NP decreases to almost zero within 40 min for Au@Ag25. This time was reduced to 22 min for Au@Ag50 and then it re-rise to 28 and 33 min for Au@Ag75 and Au@Ag100, respectively.

The catalytic reaction is achieved in large excess of $NaBH_4$ concentration as compared with that of 4-NP. So, it is suitable to consider the concentration of $BH_4^-$ is constant during the reaction. Hence, the rate constant ($K_a$) is only dependent on the concentration of 4-NP. Therefore, the rate constant is first order kinetics [28]. The reaction rate constant may be represented by the following relation:

$$-K_a t = \ln(C_t/C_0) = \ln(A_t/A_0)$$

where the concentration and absorption of 4-NP at time t are $C_t$ and $A_t$, respectively, and the concentration and absorption of 4-NP at the starting of the reaction are $C_0$ and $A_0$. The rate constant ($K_a$) can be calculated from the slop of the straight line of the graphical representation of ln ($A_t/A_0$) against the reaction time (t) which is displayed in Fig. 8.

The values of $K_a$ obtained by the slope of the fitted line in Fig.8 are $1.33\times10^{-3}$ $s^{-1}$, $3\times10^{-3}$ $s^{-1}$, $2.25\times10^{-3}$ $s^{-1}$, and $1.8\times10^{-3}$ $s^{-1}$ for Au@Ag25, Au@Ag50, Au@Ag75 and Au@Ag100, respectively. This may be discussed as follow: when the Ag shell thickness is small the catalytic reactivity is the resultant of both the activity of gold and silver. As the Ag shell becomes thicker the gold core is totally isolated from the catalytic reaction and the catalytic activity is that of Ag only. The efficiency of the catalytic reaction was found to depend on the Ag shell in such way that the rate is faster for thin shells as compared with that for thick shells.

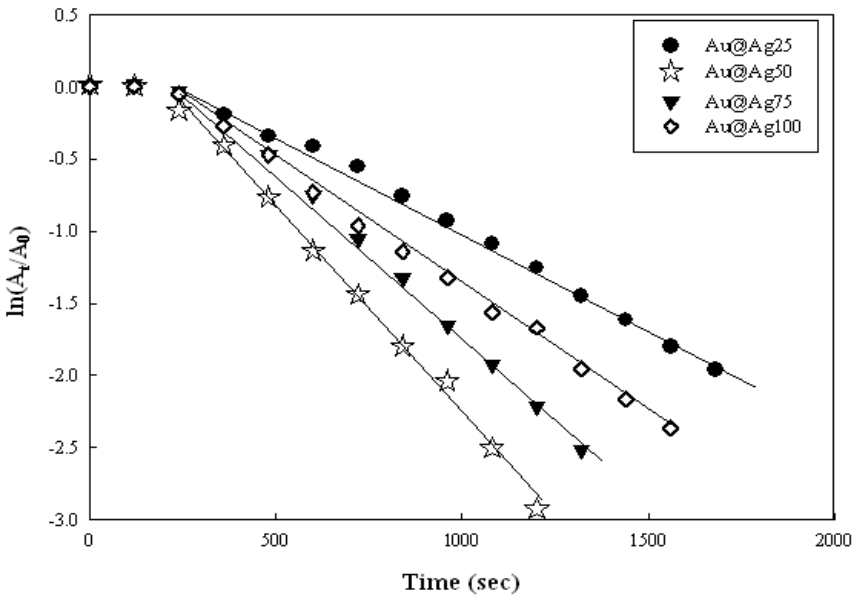


**Fig. 8 $\ln(A_o/A_t)$ vs time plot for determination of rate constants of core@shell nanoparticles with shell thickness**

## CONCLUSION

The obtained Au@Ag core@shell nanocomposites indicate a continuous increase in the Ag shell with the incremental addition of $AgNO_3$. The zeta potential measurements show the high stability of the prepared samples on aqueous solution. The designed PVP capped Au@Ag core@shell showed catalytic activity in reducing 4-NP to 4-AP in the presence of $NaBH_4$. The rate of the reaction was found to be of pseudo-first-order with respect to the 4-NP concentration.

## REFERENCES

[1] Kuroda, K., Ishida, T., and Haruta, M., *J. Molec Catalysis A*, 2009; 298, 7-11.

[2] Narayanan, K.B. and Sakthivel, N., *J. hazard. mater*, 2011; 189, 519-525.
[3] Koga, H. and Kitaoka, T., *Chem. Eng. J*, 2011; 168, 420-425.
[4] Lu, W., Ning, R., Qin, X., Zhang, Y., Chang, G., Liu, S., Luo, Y., and Sun, X., *J. hazard. mater*, 2011; 197, 320-326.
[5] Gao, S., Zhang, Z., Liu, K., and Dong, B., *Appl. Catalysis B*, 2016; 188, 245-252.
[6] Yuan, L., Yang, M., Qu, F., Shen, G., and Yu, R., *Electrochimica Acta*, 2008; 53, 3559-3565.
[7] Tojo, C. and Vila-Romeu, N., *Materials*, 2014; 7, 7513-7532.
[8] Haldar, K.K., Kundu, S., and Patra, A., *ACS Appl Mater Interfaces*, 2014; 6, 21946-21953.
[9] Yang, J., Lee, J.Y., and Too, H.P., *J Phys Chem B*, 2005; 109, 19208-19212.
[10] Sahu, P. and Prasad, B.L.V., *Colloids and Surfaces A*, 2015; 478, 30-35.
[11] Ma, Y., Li, W., Cho, E.C., Li, Z., Yu, T., Zeng, J., Xie, Z., and Xia, Y., *ACS Nano*, 2010; 4, 6725-6734.
[12] Pocurull, E., Marcé, R., and Borrull, F., *J. Chromatography A*, 1996; 738, 1-9.
[13] Karim, K. and Gupta, S., *Bioresource technology*, 2001; 80, 179-186.
[14] Marais, E. and Nyokong, T., *J. Hazard mater*, 2008; 152, 293-301.
[15] Bo, L., Zhang, Y., Quan, X., and Zhao, B., *J hazard mater*, 2008; 153, 1201-1206.
[16] Oturan, M.A., Peiroten, J., Chartrin, P., and Acher, A.J., *Environmental Science & Technology*, 2000; 34, 3474-3479.
[17] Sen, I.K., Maity, K., and Islam, S.S., *Carbohydrate polymers*, 2013; 91, 518-528.
[18] Aromal, S.A. and Philip, D., *Spectrochimica Acta A*, 2012; 97, 1-5.
[19] Eisa, W.H., Al-Ashkar, E., El-Mossalamy, S.M., and Ali, S.S.M., *Chemical Physics Letters*, 2016; 651, 28-33.
[20] Mock, J.J., Smith, D.R., and Schultz, S., *Nano Letters*, 2003; 3, 485-491.
[21] Lim, J., Yeap, S.P., Che, H.X., and Low, S.C., *Nanoscale research letters*, 2013; 8, 1-14.
[22] Tomaszewska, E., Soliwoda, K., Kadziola, K., Tkacz-Szczesna, B., Celichowski, G., Cichomski, M., Szmaja, W., and Grobelny, J., *J. Nanomaterials*, 2013; 2013, 1-10.
[23] Alexandridis, P., *Chem. Eng. Tech*, 2011; 34, 15-28.
[24] Behera, M. and Ram, S., *J Inclusion Phenomena and Macrocyclic Chemistry*, 2012; 72, 233-239.
[25] Eisa, W.H. and Shabaka, A.A., *Reactive and Functional Polymers*, 2013; 73, 1510-1516.
[26] Cui, G., Sun, Z., Li, H., Liu, X., Liu, Y., Tian, Y., and Yan, S., *J. Mater. Chem. A*, 2016; 4, 1771-1783.
[27] Mahamallik, P. and Pal, A., *RSC Adv.*, 2015; 5, 78006-78016.
[28] Chen, D., Li, J., Cui, P., Liu, H., and Yang, J., *J. Mater. Chem. A*, 2016; 4, 3813-3821.